Sustainable Hydraulics in the Era of Global Change – Erpicum et al. (Eds.)

How will be future rainfall IDF curves in the context of climate change?

H. Tabari, P. Hosseinzadehtalaei & P. Willems
Hydraulics Division, Department of Civil Engineering, KU Leuven, Belgium

S. Saeed, E. Brisson & N. Van Lipzig
Department of Earth and Environmental Sciences, KU Leuven, Leuven, Belgium

ABSTRACT: The design statistics for water infrastructures are typically derived from rainfall intensity–duration–frequency (IDF) curves which compound frequency and intensity aspects of rainfall events for different durations. Current IDF curves are constructed based on historical time series, with an underlying temporal stationarity assumption for the probability distribution of extreme values. However, climate change casts doubt on the validity of this assumption due to ongoing and projected changes in the intensity and frequency of extreme rainfall. In this study, IDF curves for historical periods obtained from the convection permitting CCLM model with spatial and temporal resolutions of 2.8 km and 15 minutes and an ensemble of climate models (CMIP5) are validated based on observations-based curves. After this validation, future climate IDF relationships are obtained based on a quantile perturbation approach. It is concluded that the sub-hourly precipitation intensities at 15 and 30 minutes in the IDF curves derived from the CCLM 2.8 km model underestimate the observed extreme rainfall intensities. For the daily intensities, less deviation is observed for both the CCLM and the CMIP5 GCM runs. Future climate projections show potentially strong changes in extreme rainfall intensities, making the historical climate based IDF design standards unsuitable for the future extreme events.

1 INTRODUCTION

Urban drainage systems, stormwater infrastructure, culverts and other hydraulic structures are designed based on specific design storms derived from rainfall Intensity–duration–frequency (IDF) curves. The IDF curves quantify the frequency of occurrence of a storm with a specific intensity at different durations. The curves are traditionally derived from historical rainfall records by making a temporal stationarity assumption of rainfall series, implying that the intensity and frequency of historical rainfall extremes remain unchanged for the future. However, the Fifth Assessment Report from the Intergovernmental Panel on Climate Change (IPCC 2013) reported that the frequency and intensity of extreme rainfall would likely increase in a warmer climate. Accordingly, an increase in these characteristics of intense rainfall has been observed over most land areas in the late 20th century (e.g., Frich et al. 2002; Madsen et al. 2009; Tabari et al. 2014). Hence, as the pattern of extreme events shifts, the expected changes and uncertainty have to be incorporated in the IDF curve construction to reduce the risk of malfunction or failure of the current infrastructures in the future. In order to examine how the intensity and frequency of heavy rainfall events will change in the future, climate model projections under current and future greenhouse gas scenarios can be applied.

Global climate models (GCMs) have been predominantly used for estimation of future modification in intense rainfall under increased greenhouse gas conditions (e.g., Mpelasoka & Chiew 2009; Tabari et al. 2015; Asokan et al. 2016). However, the spatial resolution of GCMs is hundreds of kilometers which poses limitations to the explicit simulation of mesoscale processes involved during extreme precipitation as well as to the representation of the land surface features (Frei et al. 2006; Hassanzadeh et al. 2014). The processes that cannot be resolved in horizontal grid spacing of GCMs are parameterized, which is a source of large bias and uncertainty in the simulations (Prein et al. 2013; Kendon et al. 2014; Olsson et al. 2015). A more trustworthy representation of these processes and features is provided at finer spatial resolutions of regional climate models (RCMs), dynamically derived from either GCMs or reanalysis data. The spatial resolution of RCMs is typically between 50 and 12 km, for instance 50 km for RCMs implemented and simulated in the project PRUDENCE (Christensen and Christensen 2007) and NARCCAP (Mearns et al. 2009), 25 km in ENSEMBLES (van der Linden and Mitchell 2009) and 12 km in EURO-CORDEX (Giorgi et al. 2009). Even if the spatial resolution of RCMs is much higher than that of GCMs, the grid size is still too large to adequately represent convective rain which is primary importance for urban flood risk analysis. During the past few years, considerable efforts have been made to develop climate models with spatial resolutions less than about 4 km (namely, convection permitting model) at which deep convective phenomena are sufficiently resolved, and orography and land surface are represented more realistically (e.g., Mahoney et al. 2013; Attema et al. 2014; Kendon et al. 2014; Brisson et al. 2015).

Next to the need of high spatial resolution of design storms, precipitation data with durations of less than a day and even less than an hour are required for urban hydrological applications (Willems et al. 2012; Gregersen et al. 2013). Such high temporal resolution data are rarely provided by GCMs and even if this is the case, the data are associated with large biases. Even though computationally intensive, RCMs are generally expected to provide more realistic sub-hourly rainfall series (Kuo et al. 2014). A number of studies have performed to develop future IDF curves based on either statistically downscaled rainfall series from GCMs or RCM outputs (e.g., Mailhot et al. 2007; Willems & Vrac 2011; Wang et al. 2013; Rodriguez et al. 2014; Mirhosseini et al. 2015), but there are only a few instances of sub-hourly convection permitting model use in the literature.

To address both fine spatial and temporal needs, we use sub-daily precipitation outputs from the COSMO-CLM (CCLM) model with spatial scale of 2.8 km for future IDF curves construction. In addition to the CCLM model, the IDF relationships are analyzed based on the precipitation results from an ensemble of the Coupled Model Intercomparison Project of the World Climate Research Programme – Phase 5 (CMIP5) GCMs. To the best of our knowledge, this is the first time that future IDF curves are developed based on such high spatial (i.e., 2.8 km) and temporal (i.e., hourly) resolution climate model projections and such large ensemble of GCMs (around 200 runs).

2 MATERIALS AND METHODS

2.1 *Data*

This study makes use of the new GCM outputs for daily precipitation from the CMIP5 multi-model experiment. In the dataset, future precipitation projections for the 21st century, which extend to 2100, are forced by prescribed levels of total radiative forcing, referred to as Representative Concentration Pathways (RCPs), determined by a cumulative measure of greenhouse gas emissions, land use and air pollution. Four greenhouse gas concentration scenarios namely RCP2.6, RCP4.5, RCP6.0 and RCP8.5 were used in this study. In total, the precipitation data for 194 GCM runs (historical control run, and RCP based scenario runs) from 30 climate models with spatial resolutions between 89 km and 523 km are analyzed. Table 1 lists the name of the models and the number of runs per model.

Table 1. Climate models and number of runs per model used in this study (194 runs).

	Resolution		Number of runs				
Model	Longitude (degree)	Latitude (degree)	Historical	RCP2.6	RCP4.5	RCP6.0	RCP8.5
ACCESS 1.0	1.9	1.3	1	–	1	–	1
ACCESS 1.3	1.9	1.3	1	–	1	–	1
BCC-CSM1.1	2.8	2.8	3	–	–	–	–
BCC-CSM1.1(m)	1.1	1.1	1	1	1	1	1
BNU-ESM	2.8	2.8	1	1	1	–	1
CanESM2	2.8	2.8	5	5	5	–	5
CMCC-CM	0.8	0.8	1	–	1	–	1
CMCC-CMS	1.9	1.9	1	–	1	–	1
CMCC-CESM	3.7	3.8	1	–	–	–	1
CNRM_CM5	1.4	1.4	1	1	1	–	1
CSIRO-MK3.6.0	1.9	1.9	10	10	10	10	10
FGOALS-G2	4.7	2.8	1	1	1	–	1
GFDL-CM3	2.5	2.0	2	1	1	1	1
GFDL-ESM2G	2.5	2.0	1	1	1	1	1
GFDL-ESM2M	2.5	2.0	1	–	1	1	1
GISS-E2-H	2.5	2.0	2	–	–	–	–
GISS-E2-R	2.5	2.0	3	–	2	–	–
HADGEM2-CC	1.9	1.3	3	–	1	–	1
HADGEM2-ES	1.9	1.3	1	1	–	–	–
INM-CM4	2.0	1.5	1	–	–	–	1
IPSL-CM5A-LR	3.8	1.9	4	–	3	1	3
IPSL-CM5A-MR	2.5	1.3	1	1	1	1	1
IPSL-CM5B-LR	3.8	1.9	1	–	1	–	1
MIROC-ESM	2.8	2.8	1	1	1	1	1
MIROC-ESM-CHEM	2.8	2.8	1	1	1	1	1
MIROC5	1.4	1.4	3	2	1	1	3
MPI-ESM_LR	1.9	1.9	1	1	1	–	1
MPI-ESM_MR	1.9	1.9	1	1	1	–	1
MRI-CGCM3	1.1	1.1	1	1	1	1	1
NorESM1-M	2.5	1.9	3	1	1	1	1

All historical control runs were obtained from the CMIP5 database for the period 1961–1990, and all scenario runs were considered for the future period 2071–2100.

Next to the CMIP5 GCMs, sub-daily precipitation data from a high-resolution climate model named CCLM were utilized. This model is a non-hydrostatic limited area climate model developed by the climate limited-area modeling (CLM) community. The domain for the model simulations has a large size (192 × 175 gridpoints) in order to exclude the spatial spin-up effects (Brisson et al. 2015). A three-step nesting strategy is applied with the driving data (either from ERA-Interim or EC-EARTH) forcing a domain at 25 km grid mesh size, which in turn forces an integration at 7 km grid mesh size. The integration at 2.8 km grid spacing is forced with the output from the 7 km integration. Model integrations were performed for the period 2001–2010, and a thorough evaluation of decadal statistics of precipitation, temperature and cloud characteristics was recently performed (Brisson et al. 201X). The CCLM driven by EC-EARTH was performed for the period 2000–2010 and 2060–2069 using the RCP4.5 emission scenario.

For all GCM and CCLM runs, precipitation data were extracted for the pixel covering Uccle station in Central Belgium. This was done as high quality 10-min precipitation data measured with the same instrument are available at this station for more than a century, of which the data for the period 1961–2010 are used in this study. In addition to the 10-min station observations, daily E-OBS gridded data for 27.8 km and 55.7 km were used. These gridded data were aggregated to larger pixels of 167 km and 501 km for a comparison with gridded CMIP5 GCMs.

2.2 *Methods*

The IDF curves for 1-month, 1-year and 10-year return periods and for durations from 10 minutes up to one month were developed for the control and scenario periods of the climate models as well as the observations. The IDF curves were derived based on POT extreme value statistics after calibration of two-component exponential distributions, following Willems (2000).

To project the future IDF relationships, a delta change approach was applied using the following steps:

1. Derive design precipitation of different return periods and durations for the control period;
2. Derive design precipitation of the same return periods and durations as those for the control period for the scenario period;
3. Compute change factors as the ratio of design precipitation for the scenario period over that for the control period with the same return period and durations;
4. Multiply the change factors to the design precipitation of the observations with the same return period and duration.

The procedure is summarized as the following relationship:

$$P_{(F,t)} = P_{(O,t)} \times \frac{P_{(S,t)}}{P_{(C,t)}} \qquad t = 0.083,\ 1,\ 9,\ 10 \qquad (1)$$

where $P_{(F,t)}$, $P_{(O,t)}$, $P_{(S,t)}$ and $P_{(C,t)}$ are design precipitation of return period t for the future, the observations, and the scenario and control periods, respectively.

3 RESULTS AND DISCUSSION

3.1 *Validation of climate models-driven IDF curves*

The IDF curves using the CCLM model as well as its driving GCM (EC-EARTH) and reanalysis (ERA-Interim) were constructed for the historical period (2001–2010). Figure 1 shows these IDF curves with reference to the precipitation intensities from the station and E-OBS pixel data over Uccle location (Central Belgium). For sub-hourly precipitation intensities (15 and 30 minutes), which are typically used for sewer and drainage system design, the CCLM model of 2.8 km resolution tends to underestimate the precipitation intensities. For instance, for a storm of 10-year return period and 15-min duration, this underestimation can be up to 63 mm/h. Although this underestimation may be partially due to spatial scale difference, however, in reality the IDF curves from station observations (and not gridded observations) are used for the design of hydraulic structures. For sub-daily durations (hourly, 3 hourly and 6 hourly), precipitation intensities are underestimated by almost all the CCLM model runs except for some 2.8 and 7 km runs. In the case of daily to monthly durations, the precipitation intensities simulated by the models are very close to each other. Nevertheless, it can be concluded from the IDF plot that the precipitation intensities are overestimated by the driving ERA-Interim reanalysis data and underestimated by the driving EC-EARTH GCM.

The IDF curves were also developed using the 58 control runs of the CMIP5 GCMs for the period 1961–1990 (Fig. 2). It was difficult to include the IDF curves for the gridded data with different pixel sizes equal to that of each GCM, so the IDF curves for only the upper and lower limit of pixel sizes were added to the plot in Figure 2. As shown, most of the simulated IDF curves by the CMIP5 GCMs are within the range provided by the gridded data. The GCMs' IDF curves underestimate those based on the station observations which are used in practice for hydraulic infrastructure design.

3.2 *Future IDF curves*

After validation of the IDF curves estimated by the climate models for the control period, the future IDF curves are projected based on the quantile perturbation approach (Willems & Vrac, 2011; Ntegeka et al., 2014). Instead of using this perturbation downscaling method for perturbing precipitation time series to develop the IDF curves for the future (e.g. Willems,

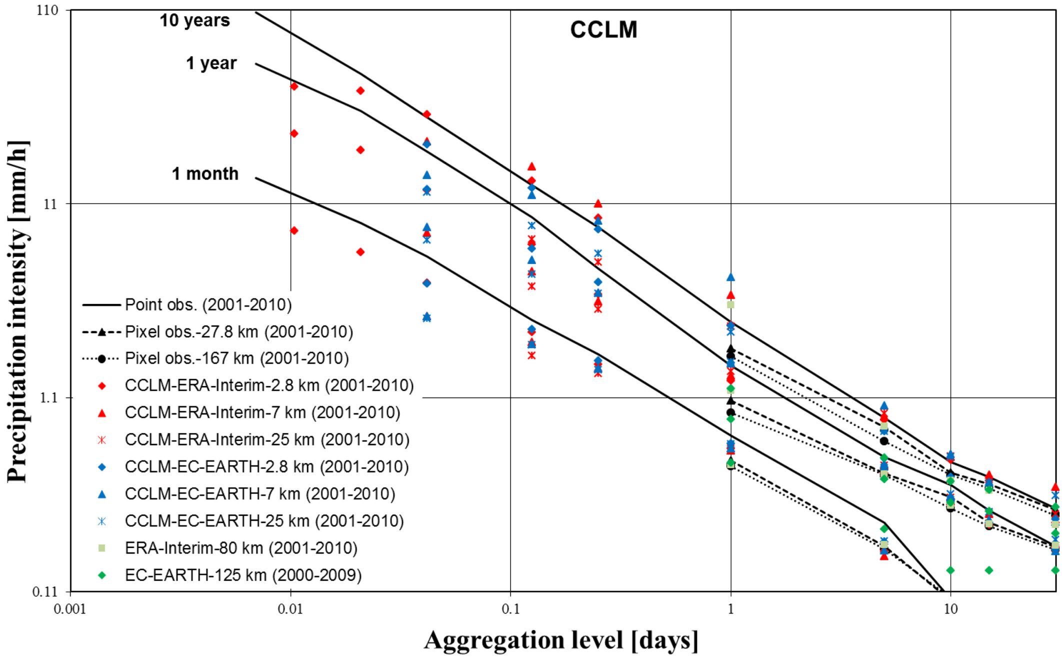

Figure 1. Baseline IDF curves using the CCLM model and its driving GCM and reanalysis versus corresponding IDF curves obtained using point and pixel observations at Uccle for the historical period 2001–2010.

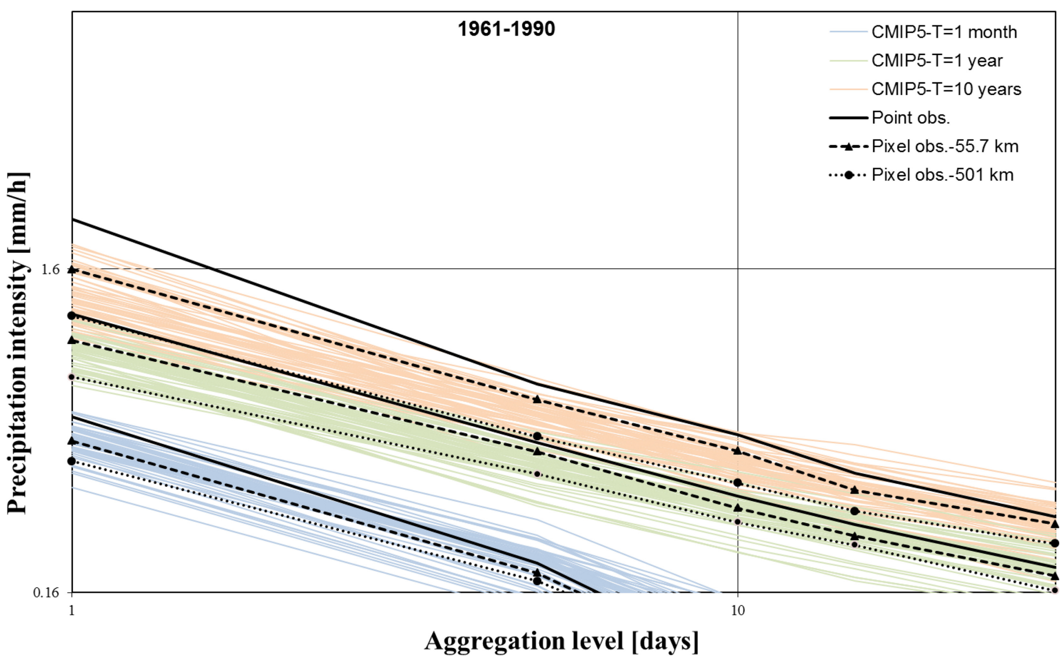

Figure 2. Baseline IDF curves using the CMIP5 GCMs versus corresponding IDF curves obtained using point and pixel observations at Uccle for the historical period 1961–1990.

2013), we perturbed design precipitation considering three aspects of precipitation (i.e., intensity, duration and frequency). The change factors in IDF relationships between the control (2000–2001) and scenario (2060–2069) runs of the CCLM model for different return periods and aggregation levels are presented in Figure 3. Both increasing and decreasing precipitation intensities are projected by the CCLM model.

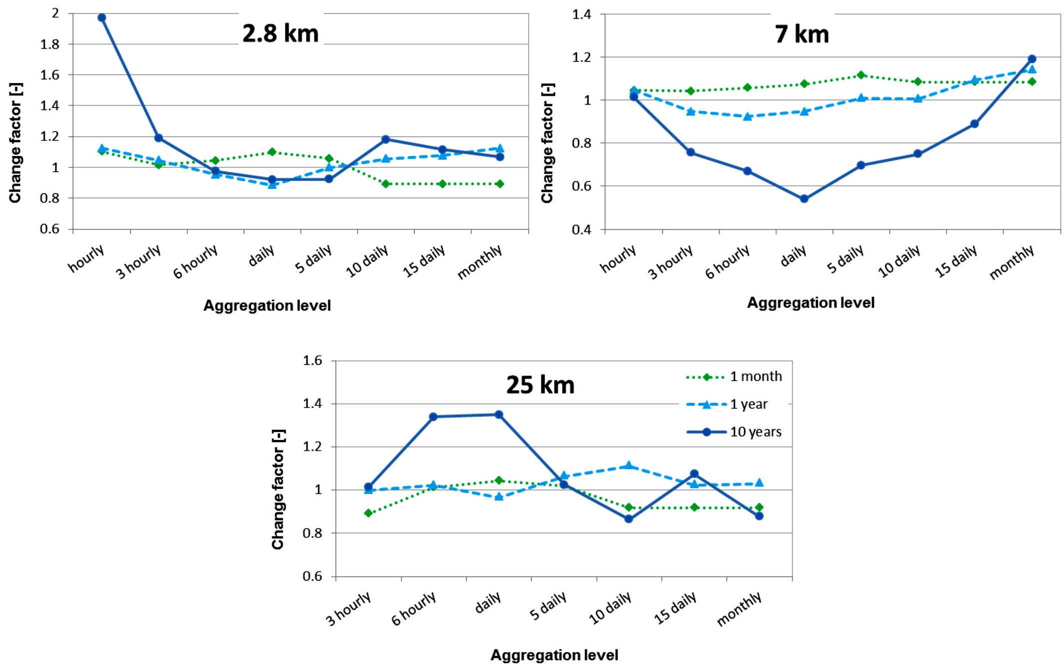

Figure 3. Relative changes in IDF relationships between the control (2000–2001) and scenario (2060–2069) runs of the CCLM model for different return periods and aggregation levels.

The most noticeable change is a 97% increase in hourly precipitation intensity for the 10-year return period by the CCLM 2.8 km model. The 46% reduction in daily precipitation intensity by the CCLM 7 km model and 34–35% increase in daily and 6-h precipitation intensities by the CCLM 25 km model are the other notable changes in IDF relationships.

The change factors for the ensemble of the CMIP5 GCMs for all RCPs (RCP2.6, RCP4.5, RCP6.0 and RCP8.5) indicate an increase in extreme precipitation intensities of 1- and 10-year return periods for all durations (Fig. 4). For the smaller 1-month return period, the increase is observed only for 1- and 5-day durations, while the other aggregation levels show a slight decrease. For the higher precipitation intensities ($T > 1$ year), the increment in design precipitation increases with decreasing duration and increasing return period. Based on the 95th percentile (median) of change factors by the GCMs, which is shown by the upper whisker (red line inside the box) in the box-plot in Figure 4, the precipitation intensity of 10-year return period and daily duration increases by 48% (15%).

The future IDF curves obtained based on the CCLM model results downscaled for the study region for three return periods ($T = 1$ month, 1 year and 10 years) and ten durations (from hourly to monthly) are shown in Figure 5. The plot shows that future IDF curves are expected to change with the future climate. The most noticeable change is seen for the hourly precipitation intensity of 10-year return period by the CCLM 2.8 km. Around 100% increase by this model implies that a hydraulic structure designed for storms of a 10-year return period will significantly be underdesigned for the future extreme events.

The future IDF curves for the end of the 21st century (2071–2100) using the CMIP5 GCMs versus the existing IDF curves (1961–1990) based on Uccle station observations are for each RCP scenario separately plotted in Figure 6. As one can see, the precipitation intensities for the future IDF curves are predominantly higher than their corresponding values for the existing IDF curves. For instance, for a 10-year return period with daily duration, a high percentage precipitation intensity increase approximately by 37%, 35%, 50% and 64% relative to the existing IDF curves is projected for the future IDF curves for the RCP2.6, 4.5, 6.0 and 8.5, respectively. This indicates that the current hydraulic structures and other water infrastructure will not be able to cope with more intense and frequent extreme events in the future. The strongest increase in extreme precipitation obtained in this study for Central Belgium using the CMIP5 GCMs is much higher than that (about 30% increase) reported by Willems & Vrac (2011) based on a set of 17 ensemble runs from the ECHAM5 general circulation model. Results are more comparable but again higher for the RCP8.5 scenario than the maximum increase of 50% reported by Willems (2013) based on an older (CMIP3) generation ensemble of 44 RCM and 69 GCM runs.

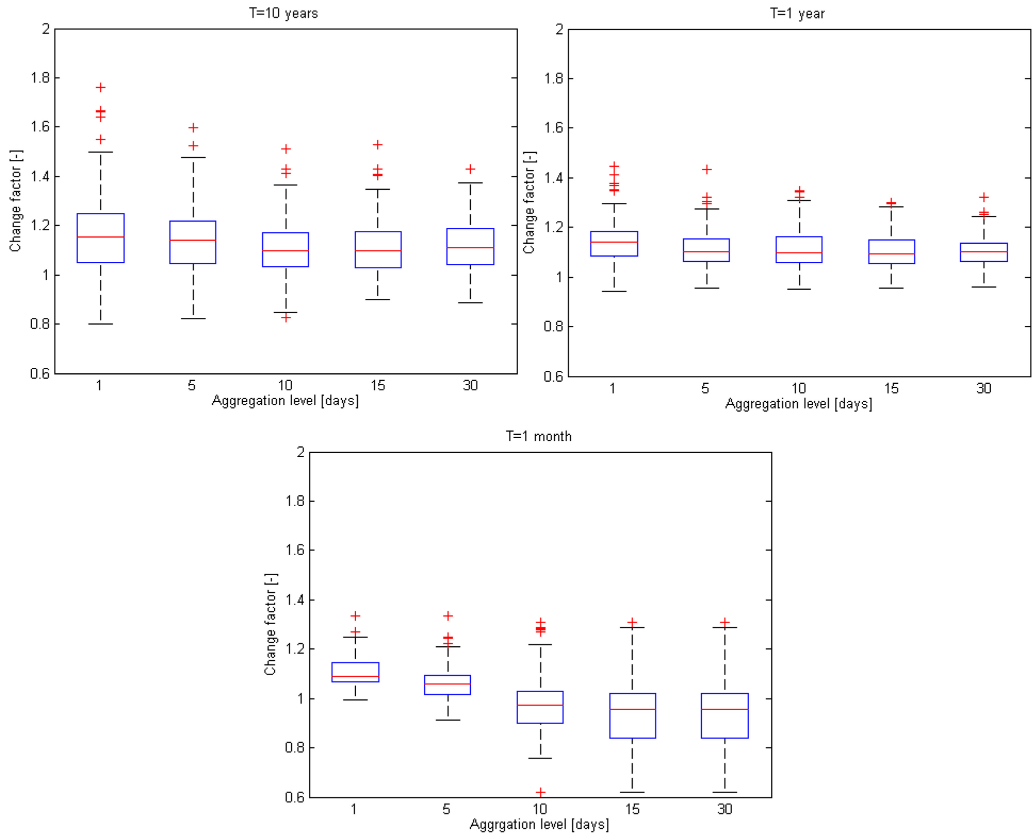

Figure 4. Relative changes in IDF relationships between the control (1961–1990) and scenario (2071–2100) runs of the CMIP5 GCMs for different return periods and aggregation levels, combining all RCPs.

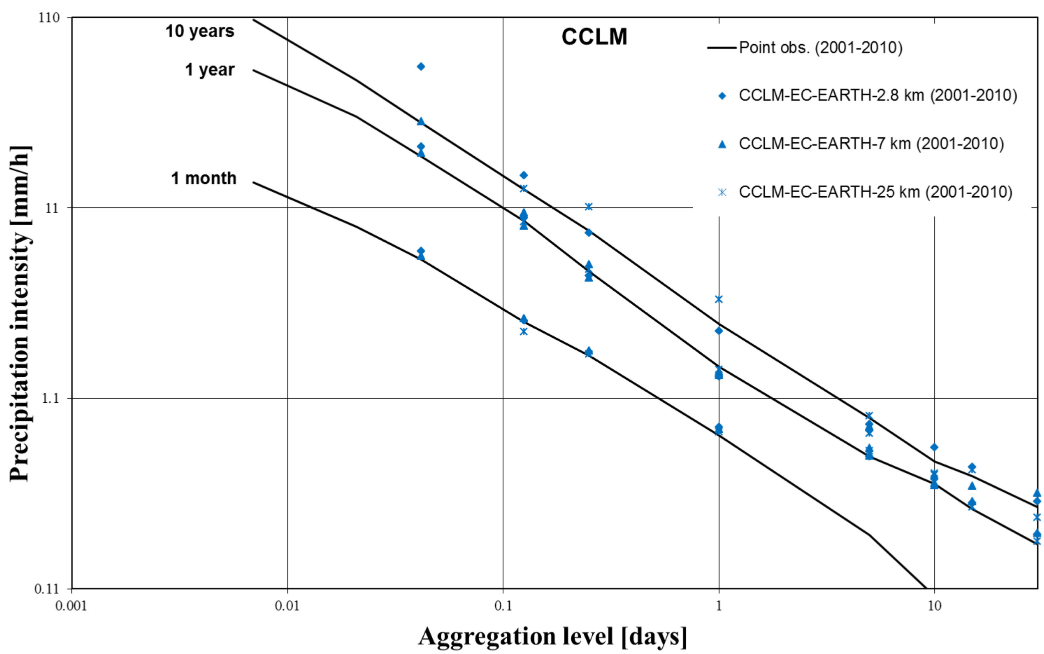

Figure 5. Future IDF curves (2060–2069) after quantile perturbation based on the CCLM model versus the historical climate IDF curves (2001–2010) at Uccle.

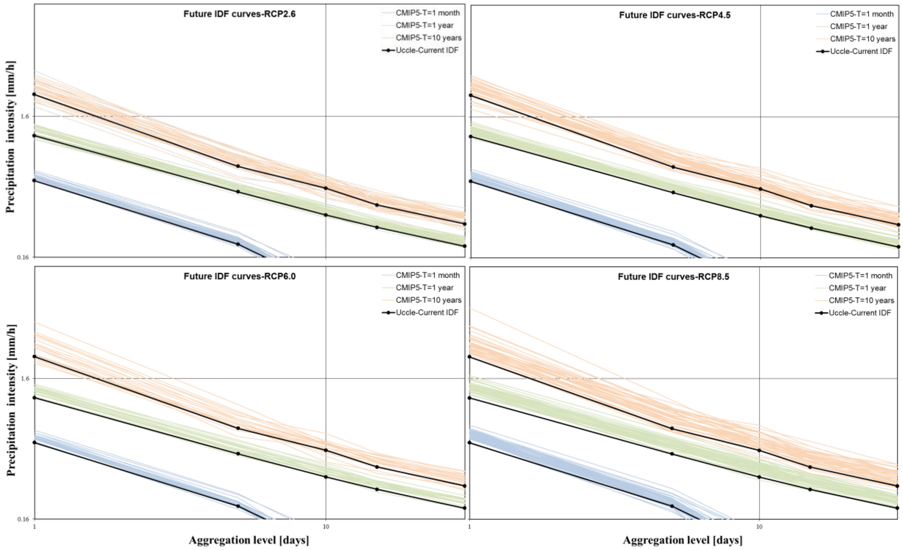

Figure 6. Future IDF curves (2071–2100) after quantile perturbation based on the CMIP5 GCMs versus the historical climate IDF curves (1961–1990) at Uccle.

4 CONCLUSIONS

This study focused on validation and future projection of IDF curves obtained from the CCLM model and a large ensemble of CMIP5 GCMs, with precipitation durations ranging between 15 minutes and one month. The future IDF curves were developed by applying climate change factors on extreme rainfall quantiles to existing IDF curves that were based on raingauge observations.. This was done to the respective durations and return periods, in the framework of a quantile perturbation downscaling approach. The results show a clear tendency of the expected extreme precipitation intensities for the future to increase. Considering the higher intensities of precipitation (T > 1 year), the amount of increase is higher for smaller time scales and larger return periods. The precipitation intensity with hourly time scale and 10-year return period may increase up to about 100%. Furthermore, the increase in the design storm intensities as derived from the CMIP5 ensemble increases with the CO_2 concentrations in the emission scenarios, ranging from 37% in the RCP2.6 scenario to 64% in the RCP8.5 scenario. The results of this study indicate that the current IDF curves are not sufficient to represent future precipitation patterns and emphasize the necessity of upgrading the curves for designing, operating and maintaining municipal water management infrastructures in the future.

ACKNOWLEDGEMENT

This study was co-financed by the Belgian Science Policy Office through the CORDEX.be project (BRAIN-be research programme).

REFERENCES

Asokan, S.M., Rogberg, P., Bring, A., Jarsjö, J. & Destouni, G. 2016. Climate model performance and change projection for freshwater fluxes: Comparison for irrigated areas in Central and South Asia. *Journal of Hydrology: Regional Studies* 5: 48–65.

Attema, J.J., Loriaux, J.M. & Lenderink, G. 2014. Extreme precipitation response to climate perturbations in an atmospheric mesoscale model. *Environmental Research Letters* 9: 014003.

Brisson, E., Demuzere, M., & van Lipzig, N.P.M. 2015. Modelling strategies for performing convection-permitting climate simulations. *Meteorologische Zeitschrift* doi:10.1127/metz/2015/0598.

Brisson, E., K. Van Weverberg, M. Demuzere, A. Devis, S. Saeed, M. Stengel, & N. P. M. van Lipzig, 201X. How well can a convection-permitting climate model reproduce decadal statistics of precipitation, temperature and cloud characteristics? *Climate Dynamics* (submitted).

Christensen, J.H., & Christensen, O.B. 2007. A summary of the PRUDENCE model projections of changes in European climate by the end of this century. *Climatic Change* 81: 7–30.

Frei, C., Schöll, R., Schmidli, J., Fukutome, S., Vidale, P.L. 2006. Future change of precipitation extremes in Europe: an intercomparison of scenarios from regional climate models. *Journal of Geophysical Research* 111, D06105, doi:10.1029/2005JD005965.

Frich, P., Alexander, L.V., Della-Marta, P., Gleason, B., Haylock, M., Klein Tank, A. M.G., & Peterson, T., 2002. Observed coherent changes in climatic extremes during the second half of the twentieth century. *Climate Research* 19: 193–212.

Giorgi, F., Jones, C., & Asrar, G. 2009. Addressing climate information needs at the regional level: the CORDEX framework. *WMO Bulletin* 58: 175–183.

Gregersen, I.B., Sørup, H.J.D., Madsen, H., Rosbjerg, D., Mikkelsen, P.S., & Arnbjerg-Nielsen, K. 2013. Assessing future climatic changes of rainfall extremes at small spatio-temporal scales. *Climatic Change* 118: 783–797.

Hassanzadeh, E., Hassanzadeh, A., & Elshorbagy, A. 2014. Quantile-based downscaling of precipitation using genetic programming: application to IDF curves in Saskatoon. *Journal of Hydrologic Engineering* 19(5): 943–955.

IPCC 2013. *Summary for Policymakers. Climate Change 2013: The Physical Science Basis*. Contribution of Working Group I to the Fifth Assessment Report of the Intergovernmental Panel on Climate Change. In: Stocker, T.F., Qin, D., Plattner, G.-K., Tignor, M., Allen, S.K., Boschung, J., Nauels, A., Xia, Y., Bex, V., Midgley, P.M.e. (Eds.).

Madsen, H., Arnbjerg-Nielsen, K., & Mikkelsen, P.S. 2009. Update of regional intensity–duration–frequency curves in Denmark: Tendency towards increased storm intensities. *Atmospheric Research* 92: 343–349.

Mailhot, A., Duchesne, S., Caya, D., Talbot, G. 2007. Assessment of future change in intensity–duration–frequency (IDF) curves for southern Quebec using the Canadian Regional Climate Model (CRCM). *Journal of Hydrology* 347: 197–210.

Mearns, L.O., Gutowski, W.J., Jones, R., Leung, L.-Y., McGinnis, S., Nunes, A.M.B. & Qian, Y. 2009. A regional climate change assessment program for North America. *EOS* 90(36): 311–312.

Mirhosseini, G., Srivastava, P., & Sharifi, A. 2015. Developing probability-based IDF curves using Kernel density estimator. *Journal of Hydrologic Engineering* 20(9): 04015002.

Mahoney, K., Alexander, M., Scott, J.D. & Barsugli, J. 2013. High-resolution downscaled simulations of warm-season extreme precipitation events in the Colorado Front Range under past and future climates. *Journal of Climate* 26: 8671–8689.

Mpelasoka, F.S., & Chiew, F.H.S. 2009. Influence of Rainfall Scenario Construction Methods on Runoff Projections. *Journal of Hydrometeorology* 10: 1168–1183.

Ntegeka, V., Baguis, P., Roulin, E., Willems, P. 2014. Developing tailored climate change scenarios for hydrological impact assessments. *Journal of Hydrology* 508C: 307–321.

Olsson, J., Berg, P., & Kawamura, A. 2015. Impact of RCM spatial resolution on the reproduction of local, subdaily precipitation. *Journal of Hydrometeorology* 16: 534–547.

Rodríguez, R., Navarro, X., Casas, M. C., Ribalaygua, J., Russo, B., Pouget, L. & Redaño, A. 2014. Influence of climate change on IDF curves for the metropolitan area of Barcelona (Spain). *International Journal of Climatology* 34: 643–654.

Tabari, H., AghaKouchak, A., & Willems, P. 2014. A perturbation approach for assessing trends in precipitation extremes across Iran. *Journal of Hydrology* 519: 1420–1427.

Tabari, H., Taye, M.T., & Willems, P. 2015. Water availability change in central Belgium for the late 21th century. *Global and Planetary Change* 131: 115–123.

van der Linden, P., & Mitchell, J.F.B. 2009. *ENSEMBLES: climate change and its impacts: summary of research and results from the ENSEMBLES project*. Met Office Hadley Centre, Exeter, 160 pp.

Wang, D., Hagen, S.C., & Alizad, K. 2013. Climate change impact and uncertainty analysis of extreme rainfall events in the Apalachicola River basin, Florida. *Journal of Hydrology* 480: 125–135.

Willems, P., Arnbjerg-Nielsen, K., Olsson, J. & Nguyen, V.T.V. 2012. Climate change impact assessment on urban rainfall extremes and urban drainage: methods and shortcomings. *Atmospheric Research* 103: 106–118.

Willems, P., 2000. Compound IDF-relationships of extreme precipitation for two seasons and two storm types. *Journal of Hydrology* 233: 189–205.

Willems, P., & M. Vrac, 2011: Statistical precipitation downscaling for small-scale hydrological impact investigations of climate change. *Journal of Hydrology* 402: 193–205.

Willems, P., 2013: Revision of urban drainage design rules after assessment of climate change impacts on precipitation extremes at Uccle, Belgium. *Journal of Hydrology* 496: 166–177.